Intact carbonic acid is a viable protonating agent for biological bases

Daniel Aminov[a], Dina Pines[a], Philip M. Kiefer[b], Snehasis Daschakraborty[b,1], James T. Hynes[b,c,2], and Ehud Pines[a,2]

[a]Department of Chemistry, Ben-Gurion University of the Negev, 84105 Beer-Sheva, Israel; [b]Department of Chemistry, University of Colorado Boulder, Boulder, CO 80309-0215; and [c]PASTEUR, Départmente de Chimie, Ecole Normale Supérieure, PSL Research University, Sorbonne Université, UPMC Université Paris 06, CNRS, 75005 Paris, France

Contributed by James T. Hynes, August 28, 2019 (sent for review June 3, 2019; reviewed by Graham R. Fleming and Sharon Hammes-Schiffer)

Carbonic acid H_2CO_3 (CA) is a key constituent of the universal CA/bicarbonate/CO_2 buffer maintaining the pH of both blood and the oceans. Here we demonstrate the ability of intact CA to quantitatively protonate bases with biologically-relevant pK_as and argue that CA has a previously unappreciated function as a major source of protons in blood plasma. We determine with high precision the temperature dependence of $pK_a(CA)$, $pK_a(T) = -373.604 + 16{,}500/T + 56.478 \ln T$. At physiological-like conditions $pK_a(CA) = 3.45$ ($I = 0.15$ M, 37 °C), making CA stronger than lactic acid. We further demonstrate experimentally that CA decomposition to H_2O and CO_2 does not impair its ability to act as an ordinary carboxylic acid and to efficiently protonate physiological-like bases. The consequences of this conclusion are far reaching for human physiology and marine biology. While CA is somewhat less reactive than $(H^+)_{aq}$, it is more than 1 order of magnitude more abundant than $(H^+)_{aq}$ in the blood plasma and in the oceans. In particular, CA is about 70× more abundant than $(H^+)_{aq}$ in the blood plasma, where we argue that its overall protonation efficiency is 10 to 20× greater than that of $(H^+)_{aq}$, often considered to be the major protonating agent there. CA should thus function as a major source for fast in vivo acid–base reactivity in the blood plasma, possibly penetrating intact into membranes and significantly helping to compensate for $(H^+)_{aq}$'s kinetic deficiency in sustaining the large proton fluxes that are vital for metabolic processes and rapid enzymatic reactions.

carbonic acid | protonation | blood plasma | biological

The idea of biological reactivity driven and regulated by enzymes and specific reactions of designed biological molecules has played a major role in biochemistry's development (1, 2). But, this perspective can overshadow important aspects of biochemical processes driven nonspecifically in the physiological environment such as reactions driven by a concentration gradient. A particular instance is the protonation reactions of bases or basic groups driven by largely homogeneous populations of either aqueous protons $(H^+)_{aq}$ (3, 4) or mobile acids such as those participating in the physiological buffer system (5, 6). Here we argue—based on experimental observations described within—that a key role in this connection is played by a previously unappreciated major proton source: carbonic acid (CA) H_2CO_3. In particular, we focus on the protonation of biorelevant bases B by CA

$$B + H_2CO_3 \underset{k_{off}}{\overset{k_{on}}{\rightleftarrows}} H^+B + HCO_3^-, \qquad [1]$$

where HCO_3^- is the bicarbonate anion (the rate constants here will be discussed within). While it deals with experiments on CA in aqueous solution, this paper focuses on the issue of the significance of CA in the blood plasma.

CA is an invariable constituent of the universal $H_2CO_3/HCO_3^-/CO_2$ buffer ("the CA buffer") which helps maintain the pH of both the blood plasma (7–9) and the earth's seas and oceans (10–15). The CA buffer constitutes about 83% of blood plasma's buffer capacity and about 53% of the whole blood capacity (16, 17) and, as the blood's "front-line" buffer, is extremely important for human physiology (7, 8). It is regulated in the body by one of nature's most efficient enzymes, carbonic anhydrase (18, 19). It is crucial that the very large HCO_3^- concentration (26 through 28 mM) (1, 2, 7–9) in equilibrium with CA makes CA a permanent factor in the plasma, with an equilibrium 2–3 μM concentration, about 70× larger than $[H^+]_{aq}$. Finally, the CA buffer is a critical respiratory system component, responsible for CO_2 transport across membranes (5, 6, 9, 20, 21).

CA's chemistry is dominated by its spontaneous breakdown (22) in bulk water into CO_2 and H_2O

$$H_2CO_3 \underset{k_{CA}}{\overset{k_{dc}}{\rightleftarrows}} H_2O + CO_2, \qquad [2]$$

with a first-order decomposition reaction rate constant k_{dc} [corresponding to a decomposition lifetime $\tau_{dc} = 1/k_{dc}$ of about 60 ms (20 °C)], which is about 300× larger than the pseudo–first-order back-hydration rate constant k_{CA} (23–28). CA decomposes via a proton chain mechanism in aqueous solution—and even in the gas phase in the presence of a single water molecule (29–34).

The reverse reaction in Eq. **2**—CO_2 reacting with water to form H_2CO_3—is bimolecular, dependent on the CO_2 concentration,

Significance

The paper demonstrates the previously unappreciated feature that, despite its instability, carbonic acid (CA) acts as an effective protonating agent consistent with its pK_a value, which is here accurately determined over the full physiological temperature range. The equilibrium concentration of CA in the blood plasma is about 70× larger than $(H^+)_{aq}$, and, given CA's acidic reactivity established here, it is concluded that, in contrast to current thought, CA should be considered a far more important protonation agent in the blood than is $(H^+)_{aq}$. These conclusions should be also considered when evaluating conditions resulting in CA concentration increase, such as acidosis in the physiological context and the gradual acidification of the oceans in the environmental setting.

Author contributions: E.P. designed and initiated research; D.A., D.P., P.M.K., S.D., and J.T.H., and E.P. performed research; D.A., D.P., and E.P. analyzed data; D.P. performed kinetic analysis; and J.T.H. and E.P. wrote the paper.

Reviewers: G.R.F., University of California, Berkeley; and S.H.-S, Yale University.

The authors declare no competing interest.

[1]Present address: Department of Chemistry, Indian Institute of Technology (IIT) Patna, Bihta, Patna 801106, India.

[2]To whom correspondence may be addressed. Email: chynes43@gmail.com or epines@bgu.ac.il.

This article contains supporting information online at www.pnas.org/lookup/suppl/doi:10.1073/pnas.1909498116/-/DCSupplemental.

First published September 30, 2019.

and is the cause of CA's small equilibrium concentration in aqueous solution. CA's aqueous solutions are slightly acidic through the CA reversible proton dissociation reaction

$$H_2CO_3 \underset{k_{D(BC)}}{\overset{k_{dis(CA)}}{\rightleftarrows}} (H^+)_{aq} + HCO_3^-. \quad [3]$$

Here $k_{dis(CA)}$ is CA's overall acid dissociation rate constant and $k_{D(BC)}$ is the diffusion-limited rate constant of the back protonation of HCO_3^- to reform CA (23–26). In physiological systems, $k_{dis(CA)}$ and $k_{D(BC)}$ depend on the particular environment, with CA's equilibrium constant $K_a(CA) = k_{dis(CA)}/k_{D(BC)}$. (In the blood, the carbonic anhydrase enzyme likely accelerates regeneration of CA (18, 19), otherwise regenerated via uncatalyzed reaction (2) and protonation of HCO_3^-, Eq. **3**). The enzyme carbonic anhydrase just mentioned catalyzes Eq. **2** reactions with very high turnover of 10^4 to 10^6 CO_2 molecules per second (21). It thereby helps regulate the blood plasma's pH and CA levels, and—with the very large HCO_3^- concentration (26 through 28 mM) (1, 2, 7–9) in equilibrium with CA—makes the CA concentration an undiminished permanent factor in the blood plasma with a 2 to 3-μM equilibrium concentration.

In the context of human physiology, the importance of resolving the physiological role of CA stems from this relatively high steady-state concentration of CA, which is about 70× larger than that of $(H^+)_{aq}$ (7, 8), its potential considerable reactivity as a moderately strong carboxylic acid, and from the physiological demand for fast in vivo acid–base reactivity. In particular, this demand is absolutely vital to sustain life processes, but it appears to be inconsistent both with the hydrated proton's diminished concentration, $[(H^+)_{aq}] = 40$ nM in the blood plasma (7, 8), and with $(H^+)_{aq}$'s reduced diffusivity in biological environments due to impairment of the Grotthuss proton transport mechanism by various hydrophobic entities (35).

In order to demonstrate that CA's presence significantly eases this problem, we must first determine whether CA's instability fatally compromises—as traditionally thought—its chemical reactivity as a sufficiently strong acid of considerable protonation ability. We will argue within that CA's acid–base reactivity Eq. **1** is not so compromised. The main question here is whether CA is capable of protonating bases by one or both of the standard carboxylic acid–protonation mechanistic routes (discussed within) (36–39), or instead decomposes to H_2O and CO_2, either via Eq. **2** (23–26) or via a base-catalyzed variant

$$B + H_2CO_3 \underset{k_{CA}}{\overset{k_{ic}}{\rightleftarrows}} B + CO_2 + H_2O, \quad [4]$$

in which maximum value of k_{ic} is reached when the reaction is assumed to be diffusion-controlled, $k_{ic} = k_{D(B)}$ (36–39). Returning to Eq. **1**, it is essential for the physiological problem's solution that we will address it via the determination of how efficiently CA protonates bases—if CA acts like a standard Brønsted acid (40), i.e., via standard protonation routes mentioned above—and if that protonation is sufficiently rapid to supply protons on typical relevant biological timescales.

In the remainder of the paper, we first establish that CA behaves thermodynamically, vis-à-vis its acid equilibrium constant, like any ordinary carboxylic acid such as acetic and formic acids (40). We then demonstrate and analyze CA's kinetic ability to protonate physiological-like bases, and in particular that this protonation dominates decomposition to H_2O and CO_2. Finally, we analyze the protonation by CA's reaction kinetic mechanisms associated with Eq. **1** and demonstrate that this must in fact be much more efficient—and hence much more physiologically important—than protonation by $(H^+)_{aq}$. With these results, we offer a solution for the above-mentioned major physiological conundrum of the kinetic "deficiency" of $(H^+)_{aq}$ (7, 8).

Results and Discussion

CA pK_a Temperature Dependence. To establish that CA behaves as an ordinary protonating (Brønsted) carboxylic acid in a thermodynamic perspective, we determine its pK_a temperature dependence. The 20 °C value pK^0_a of intact CA in equilibrium with its HCO_3^- deprotonated form has been recently determined to be about 3.5 (41, 42) at zero ionic strength I = 0 and—as we now report—is about 3.6 (I = 0) at the physiologically important 37 °C, cf. Fig. 1. The reported data are obtained via temperature-dependent stopped-flow experiments (*SI Appendix*, section S7 and Fig. S4).

These key data provide the acid dissociation's important thermodynamic enthalpy and entropy parameters ΔH and ΔS, related to K_a via (43)

$$\Delta G = -RT\ln K_a, \quad \frac{d\ln K_a}{dT} = \frac{\Delta H}{RT^2}, \quad [5]$$

with R the gas constant and T the temperature in K at 1 bar pressure.

The data in Fig. 1 are well fit by

$$pK_a(T) = -373.604 + 16{,}500/T + 56.478\ln T, \quad [6]$$

which allows an excellent estimation of pK_a (CA) in the full physiological range of body temperatures from extreme hypothermia to extreme hyperthermia conditions (about 25 to 44 °C) (44–49). Further, Eqs. **5** and **6** provide the CA dissociation reaction's standard enthalpy and entropy change at 25 °C as −1.5 kcal/mol and −21.2 cal/mol/K, respectively. All of this classes CA as an ordinarily behaved carboxylic acid such as acetic and formic acids: as do they, CA shows a pK_a minimum about room temperature, in the CA case at 19 °C = 3.51 ± 0.02 and exhibits small enthalpy ΔH^o and large entropy ΔS^o changes upon

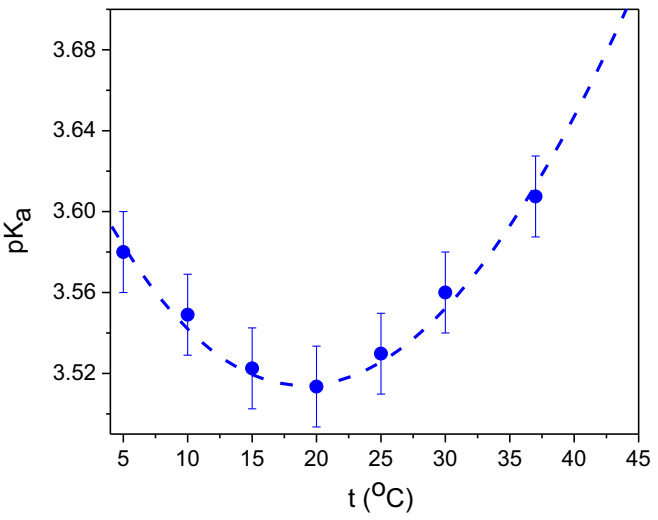

Fig. 1. Temperature dependence of the pK_a of CA. CA's pK_a was measured in the 5 to 37 °C range using a 1-stage stopped-flow arrangement (27) (*SI Appendix*, Fig. S4) with CA generated within about 1 ms by mixing equal amounts of sodium bicarbonate ($NaHCO_3$) and hydrochloric acid (HCl). The solution's pH was determined by the absorption change of 2,4-dinitrophenol (DNP) ($pK_a = 4.07 \pm 0.02$ at 20 °C), with its value's T dependence accurately known (44). Points are the averaged pK_a values of at least 5 independent experiments; the solid line is the fit to Eq. **6**. pK_a values were found (*SI Appendix*, Eq. S7.1) and then extrapolated to I = 0. Error bars directly determined from the experimental result's total spread are ±0.02 pK_a units.

proton dissociation (44–49). Our measurements give CA's dissociation free energy $\Delta G^o = \Delta H^o - T\Delta S^o = -1.5$ kcal + 6.3 kcal = 4.8 kcal at T = 298 K [pK_a(CA) = 3.52 ± 0.02 at 25 °C]; it is noteworthy that ΔG^o (CA) is dominated by the $T\Delta S^o$ contribution, another similarity to the stable carboxylic acids (44–49). In conclusion, in this thermodynamic perspective, CA behaves just like an ordinary carboxylic acid.

Well-known empirical thermodynamic-kinetics correlations (41, 42, 50–53) would strongly suggest, given the above thermodynamic results, that CA also behaves kinetically as a standard carboxylic acid. But, the experimental kinetic character of CA's base protonation ability is in fact currently unknown, and thus requires it be determined, as we now report.

Testing the Kinetic Viability of CA as a Protonating Agent. We now turn to the required experimental test of whether—in accordance with its substantial acidity predicted by its thermodynamic K_a value—CA kinetically protonates bases via Eq. **1** involving the rate constants k_{on} and k_{off} (*SI Appendix*, Eqs. S3.1–S3.3) for overall base protonation by intact CA and the deprotonation of BH^+ by HCO_3^-, respectively.

For this purpose, we selected 2 oxygen bases with structures and pK_as relevant to biological systems: the HPTS base 8-hydroxy-1,3,6-trisulfonate anion, and the 1N4S base 1-naphthol-4-sulfonate anion. The pK^o_as (I = 0) of these 2 bases' conjugate Brønsted acids (H^+Bs) are 7.95 and 8.2, respectively (54, 55). HPTS and 1N4S have basicity similar to that of many important physiological bases such the amine groups in small peptides, the hydroxyl group in tyrosine, and the imine group in histidine, whose conjugate acids' pK^o_as all fall in the range of 8 ± 2 (56). This range makes all these bases' conjugate acidity at least 3 pK_a units weaker than CA's, which indicates (*vide infra*) that their protonation by CA should be fast, approaching the diffusion limit.

Turning to the actual experiments, we have conducted stopped-flow experiments utilizing a 2-stage rapid mixing procedure. In the first cell, CA was generated by a rapid quantitative acidification by HCl of a prechosen fraction of the bicarbonate anion HCO_3^- concentration, generating the bicarbonate/CA buffer solution at the desired composition. Following a variable incubation (waiting) time τ_{inc} during which a CA partial loss occurs via the spontaneous decomposition Eq. **2**, the resulting CA solution was mixed in the second cell with the base solution, allowing CA's protonation. Fig. 2 shows the protonated base fraction versus τ_{inc}.

For each base B in Fig. 2, the measured protonated base B^+H concentration decreases with a time constant practically equal to that of the independently measured decomposition lifetime of CA (Eq. **2**). Thus, the extent of progress of the bases' protonation yields appears to depend solely on the incubation time of CA, which in turn determines the amount of intact CA left at the time of mixing with the base solution. The behavior of the protonated base concentration's reduction with longer incubation time in Fig. 2 directly reflects CA's prior decay via Eq. **2** unaltered by any further kinetic process. This observation leads to an important conclusion: CA's protonation of the base proceeds without any CA concentration decomposition loss beyond that which occurred during the incubation time.

The conclusion just stated also implies that the CA's base protonations' timescale is much shorter than CA's time for decomposition—occurring within the mixing time of the stopped-flow apparatus of about 1 ms—the central conclusion; thus the protonation reaction occurs practically instantaneously compared to both the decomposition and mixing timescales. This is confirmed by the full numerical solutions of the rate equations for the kinetic scheme for CA's time development. This scheme accounts for all our report's reactions, and is numerically solved for the aqueous solution concentrations of the key species H_2CO_3, HCO_3^-, H^+, and B; it includes reaction Eqs **2** and **4** as

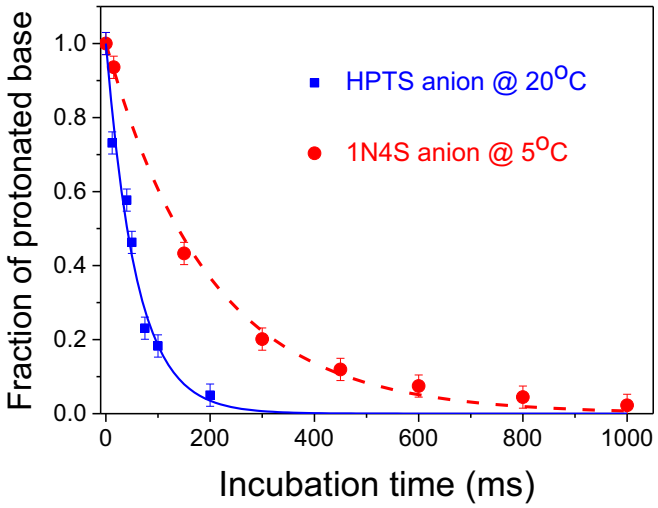

Fig. 2. Fraction of protonated base (anions of HPTS and 1NS4) versus incubation time $\tau_{inc.}$ Time dependence of the experimentally observed fractions (points) of the anionic bases HPTS and 1NS4 protonated by CA vs. the incubation time τ_{inc}, the time elapsed from the moment CA was generated by HCl–bicarbonate reaction until it is mixed (duration τ_{mix} until the solution is homogeneous) with the base solution (see *Methods* for experimental setup description). During incubation, the CA concentration decreases continuously with a temperature-dependent exponential lifetime τ_{dc} (solid and dashed lines) due to its spontaneous decomposition via Eq. **2**. τ_{dc} is independently determined to be on the 10s of milliseconds timescale by standard stopped-flow experiments (*SI Appendix*, Fig. S4) (27, 28). The protonated base fraction decreases with increased τ_{inc} because of CA's spontaneous decomposition. Protonation is evidently spontaneous and much faster than τ_{mix} and τ_{dc} timescales (see text).

well as those for the 2 CA protonation mechanisms mentioned in the Introduction.

As part of this full kinetic scheme we analyze the overall protonation reaction by CA Eq. **1** in terms of 2 standard protonation routes. The first is a direct protonation route R_d, with contact protonation occurring according to (36–39)

$$H_2CO_3 + B \underset{k_S}{\overset{k_{D(B)}}{\rightleftarrows}} [B\cdots H_2CO_3]_a \xrightarrow{k_p} H^+B + HCO_3^-, \qquad [7]$$

which includes diffusive complex formation/dissociation prior to the protonation step. $k_{D(B)}$ are the reactants' diffusion-limited rate constants and k_S is the diffusion-limited rate constant for separating the products from contact to bulk. k_p is the rate constant for the unimolecular (contact) protonation. We estimate its magnitude from free-energy correlations; see *SI Appendix* for details [the very slow back-protonation of bicarbonate anion to reform CA is neglected (26)]. R_d is the main base protonation route for bimolecular protonation by weak acids, whose acid dissociation rate is not large compared to their bimolecular base-encounter rate.

The standard second pathway is an indirect protonation route R_i, in which the acid first dissociates to produce a hydrated proton $(H^+)_{aq}$, which then protonates the base (36–39)

$$H_2CO_3 + B \underset{k_{D(BC)}}{\overset{k_{dis(CA)}}{\rightleftarrows}} (H^+)_{aq} + B + HCO_3^- \underset{k_{dis(HB)}}{\overset{k_{D(HB)}}{\rightleftarrows}} HCO_3^- + H^+B, \qquad [8]$$

with $k_{D(BC)}$ and $k_{dis(CA)}$ defined as in Eq. **3**. This route involves the diffusive recombination of ions to reform CA and the

diffusive base-aqueous proton encounter to form H^+B. In Eq. **8**, $k_{dis(HB)}$ is the H^+B's acid dissociation rate constant and $k_{D(HB)}$ is the diffusion-limited rate constant of the back protonation of B to reform H^+B. R_i is the main protonation route for strong, i.e., readily dissociating, acids.

Generation of Kinetic Plots in Fig. 3. We now ask—in connection with our experimental results for CA's protonation viability shown in Fig. 2—which of CA's 2 protonation routes—direct R_d or indirect R_i—is more important. We also check the possibility of the base catalyzing the decomposition of CA before it is able to protonate the base, the R_{ic} route with the k_{ic} second-order reaction rate constant (compare Eq. **4**). This is accomplished by numerically solving the following set of rate equations covering the CA-base kinetic scheme described above:

$$\begin{aligned} d[H_2CO_3]/dt &= -k_{on}[H_2CO_3][B] + k_{off}\left[HCO_3^-\right][H^+B] + k_{D(BC)} \\ &\left[HCO_3^-\right][H^+] - k_{dis(CA)}[H_2CO_3] - k_{ic}[H_2CO_3][B] - k_{dc}[H_2CO_3] \\ d\left[HCO_3^-\right]/dt &= k_{on}H_2CO_3][B] - k_{off}[HCO_3][H^+B] - k_{D(BC)} \\ &\left[HCO_3^-\right][H^+] + k_{dis(CA)}[H_2CO_3] \\ d[H^+]/dt &= -k_{D(HB)}[H^+][B] + k_{dis(HB)}[H^+B] - k_{D(BC)}\left[HCO_3^-\right][H^+] \\ &+ k_{dis(CA)}[H_2CO_3] \\ d[B]/dt &= -k_{on}\left[H_2CO_3\right][B] + k_{dis(HB)}\left[H^+B\right] + k_{off}\left[HCO_3^-\right][H^+B] \\ &- k_{D(HB)}[H^+][B] \end{aligned} \quad [9]$$

(We have neglected the reaction $CO_2 + OH^- \rightleftarrows HCO_3^-$ since the OH^- concentration will be negligible in the strongly acidic pH ~3.5 experimental solutions.)

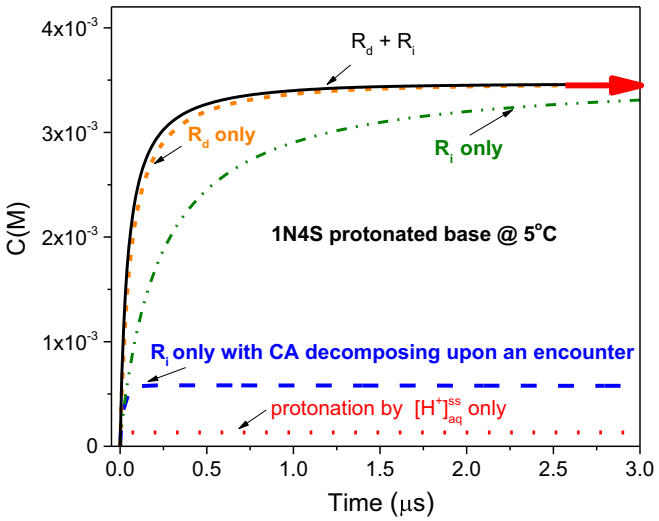

Fig. 3. Calculated kinetic profiles of the rise of the absorption of protonated 1N4S base via the numerical solution of Eq. **9**. The simulated kinetic profiles are compared with the experimental absorption signal of 3.7 mM 1N4S after mixing with 1:1 3.5 mM buffer solution of CA/HCO^-_3. Red arrow: the stopped-flow experiment's observed protonated base concentration after mixing with CA. The arrow also marks the predicted protonated base's concentration assuming full quantitative protonation by CA. Solid line: Both R_d (Eq. **7**) and R_i routes (Eq. **8**) of the base protonation are active. Dotted line: Protonation by $(H^+)_{aq}$ without participation of any CA protonation reactions. The indirect protonation via $(H^+)_{aq}$ is treated as diffusion-limited (*SI Appendix*, section S4). Dashed line: assuming that CA indirectly, but not directly, protonates the base and decomposes upon encountering a base molecule according to Eq. **4**. Dot-dot-dashed line: assuming only the indirect protonation route R_i. Short-dashed line: solution assuming only the direct protonation route R_d; this is almost indistinguishable from the solid line where both CA's direct and indirect protonation routes R_d and R_i are active. Similar analysis and conclusions apply for the HPTS base (*SI Appendix*, section S3).

For the various rate constants in this reaction listing, the diffusion-controlled rate constants $k_{D(B)}$, $k_{D(BC)}$, $k_{D(HB)}$ and the rate constants k_{off}, $k_{dis(CA)}$, and $k_{dis(HB)}$ for the direct route parameters and for the indirect route parameters are available (*SI Appendix*, Tables S1 and S2, respectively). The unimolecular rate constants' values for CA decomposition to H_2O and CO_2 are k_{dc} (20 °C) = 19.5 s^{-1} and k_{dc}(5 °C) = 5.5 s^{-1}, determined independently by conventional 1-stage stopped-flow experiments (*SI Appendix*, section S7).

The first conclusion is that, as noted above, the full numerical solutions of the kinetic scheme rate Eq. **9** set confirm the conclusions we previously reached for Fig. 2. The detailed mechanistic question requires a bit more analysis. The relatively long timescale of the Fig. 2 experiments cannot directly provide the reaction mechanisms for the too-rapid protonation time dependence; nonetheless, our kinetic scheme provides such mechanistic information by comparing the scheme's predictions for the limiting protonated base concentration value reached in the experiments. The detailed kinetic protonation profile results for assorted mechanistic possibilities displayed in Fig. 3 for the 14NS base [and also for the HPTS base (*SI Appendix*, Fig. S3)] show by this comparison (compare the red arrow in Fig. 3) that the direct protonation route R_d dominates the protonation reaction, and—more generally and importantly—that the base protonation by CA must be fast compared to the decomposition to H_2O and CO_2, Eq. **2**—which can be neglected—and further, that there is negligible base-induced decomposition via Eq. **4**.

Fig. 3 contains even further information concerning CA's protonation ability and mechanisms. We first note that the Fig. 2 experimental protonation yield (with respect to intact CA's initial concentration) approaches 100%; thus, practically all of the CA acidic protons were transferred to the base, quantitatively protonating it. As mentioned above, the Fig. 3 calculations show that the direct protonation R_d route largely dominates over the indirect protonation route R_i (assuming R_d is diffusion-limited), consistent with the behavior of any Brønsted acid of CA strength protonating a strong base. This domination means that under Fig. 2's conditions, the intact CA-base encounter is much faster than the encounter between the base and those $(H^+)_{aq}$ protons generated by CA dissociation. It further means that CA's direct protonation of the base largely precedes its proton dissociation, Eq. **3**; thus, the important conclusion is that most protonation reactions in our experiments have occurred by intact CA.

Fig. 3 displays other reaction possibilities. In the more significant one of these, we consider the potential "short circuiting" of R_d by the CA-B encounter route Eq. **4**, where intact CA does not protonate the base, and the encounter instead results in CA decomposing to CO_2 and H_2O. Fig. 3 indicates that this mechanism may only account for about 17% of the observed protonation yield. In view of this and the remaining Fig. 3 calculation results, as well as the discussion of the experimental Fig. 2, we can conclude that it is highly unlikely that CA appreciably decomposes as a result of encountering a base.

It is worth mentioning that our CA protonation rate constant observations are in complete harmony with our detailed ab initio CA protonation reaction mechanism, which predicts ultrafast protonation rates of strong nitrogen bases without any base-induced CA decomposition (57, 58). Specifically, Car–Parrinello molecular dynamics simulations in an aqueous environment demonstrated that CA's protonation of methylamine base CH_3NH_2 within a hydrogen (H)-bonded complex occurs extremely rapidly: The path for the practically barrierless PT from CA to methylamine within such a complex was fully mapped and the computed extremely short timescale (33–75 fs) protonation occurred without CA decomposition. The PT process is strongly downhill in free-energy character ($\Delta pK_a \sim 7$), consistent with the current assessments of the pK_a values of 3.5 (42) and 10.6 for CA and protonated methylamine, respectively (57, 58). Further, in

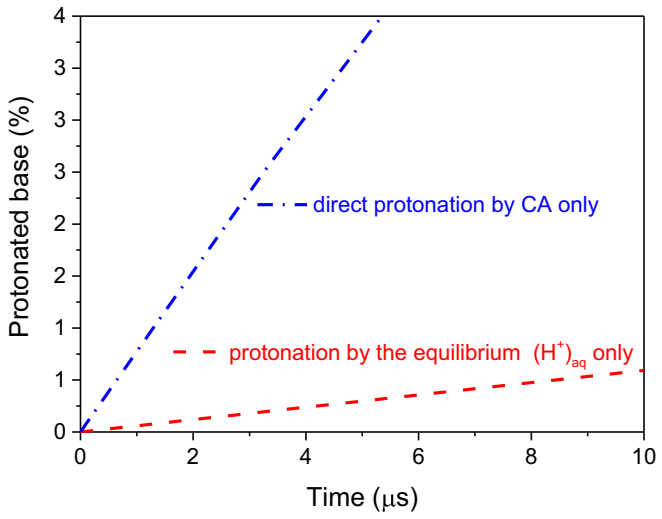

Fig. 4. Transient protonation profiles of a histidine-like base (59) B [pK_a (H^+B) = 6.0] in the presence of the CA/bicarbonate buffer. The 2 protonation reaction profiles are for the direct protonation reaction R_d by CA, $H_2CO_3 + B \rightarrow HCO_3^- + H^+B$ and for protonation by the equilibrium $(H^+)_{aq}$ protons, $(H^+)_{aq} + B \rightarrow H^+B$, assuming unidirectional protonation (since on the low-microsecond timescale the opposite reactions are not significant). Calculated using $k_{D(B)} = 3\times 10^9\ M^{-1}\cdot s^{-1}$ and $k_{D(HB)} = 1.5 \times 10^{10}\ M^{-1}\cdot s^{-1}$, for the physiological-like conditions pH = 7.4, $[HCO_3^-]$ = 25 mM, $[H_2CO_3]$ = 2.6 μM, and [B] = 10 nM. Profiles are displayed only up to the time that the protonated base reaches its steady-state concentration at the physiological pH = 7.4. The initial direct protonation rate by the CA buffer is about 12× larger than the initial protonation rate by $(H^+)_{aq}$.

additional studies we have found similar PT reaction rates when CA and the base are bridged by a single H-bonded water molecule.

Relevance for Human Physiology and Marine Biology. The present experimental studies have substantial relevance for human physiology, and their consequences are clear. Our findings, supported by previous theoretical results, demonstrate that intact CA is an efficient protonation agent and unequivocally justify the inclusion of CA as a key factor in the physiological "bookkeeping" of available protons in the blood plasma acting as an essential (reversible) part of the bicarbonate/CO_2 buffer. This inclusion of intact CA as an important physiological ingredient in the bicarbonate/CO_2 buffer addresses the important physiological problem described in the Introduction: it enables the significant bridging of the reactivity gap between the fast protonation rates needed to maintain many physiological processes and the insufficient supply of hydrated protons present at the normal physiological pH = 7.4.

Our results indicate that maintenance of the CA concentration within the normal physiological 2–3-μm range is sufficient for CA—either directly or nondirectly (by H^+ generated by CA's dissociative PT to the water solvent)—to perform several key functions. CA will not only assist maintaining the physiological pH balance; it will also directly protonate practically any nearby physiological base (either neutral or negatively charged) which requires transient protonation in order to effect its biological activity. In this connection, Fig. 4 displays—using the model reaction scheme equations described in its legend—the nonenzymatic protonation of a histidine-like residue by either the steady-state concentration of $(H^+)_{aq}$ in physiological-like conditions or directly by intact CA. [Histidine residues serve as proton "antennas" in biological environment, collecting protons and then transferring them to a reaction center; compare His-64 in the carbonic anhydrase complex (59).] Although the actual protonation rates will be affected by the specific local conditions of the blood plasma, there is a clear message of Fig. 4: that protonation by intact CA is much faster than protonation by $(H^+)_{aq}$ and, in consequence, that efficiently fast protonation reactions in biological environments are not necessarily enzymatic. This last conclusion does not follow for protonation solely by $(H^+)_{aq}$, which at its physiological steady-state concentration of 4×10^{-8} M will have typical protonation times in the millisecond range.

The situation is similar for marine biology. In the oceans, the pH is even higher than in the blood, about 8.05 compared to 7.40, and the bicarbonate concentration is also substantial, about 2 mM. Consequently, the CA concentration is 2 to 3 times larger than $[H^+]_{aq}$ there and provides the stable pH conditions upon which most marine life's well-being depends (10–15). Comprehension of intact CA's chemistry will be necessary to assess the full impact on marine life of ocean acidification driven by atmospheric CO_2 concentration increase (12, 13). Marine organisms with a calcium skeleton such as corals illustrate the issues here. Such skeletons structurally weaken when the oceans become more acidic (14, 15). Taking CA into account will approximately double the ocean acidification effect of $(H^+)_{aq}$ alone (15). Such additional contributions of CA will undoubtedly increase the projected negative effect of ocean acidification on marine life.

Conclusions

The present work indicates that CA is an important factor in the body's ability to maintain the large fluxes of protons and high protonation rates which are absolutely vital to sustain metabolic life-supporting processes and rapid enzymatic reactions. In particular, our findings identify CA as a significant source of protons

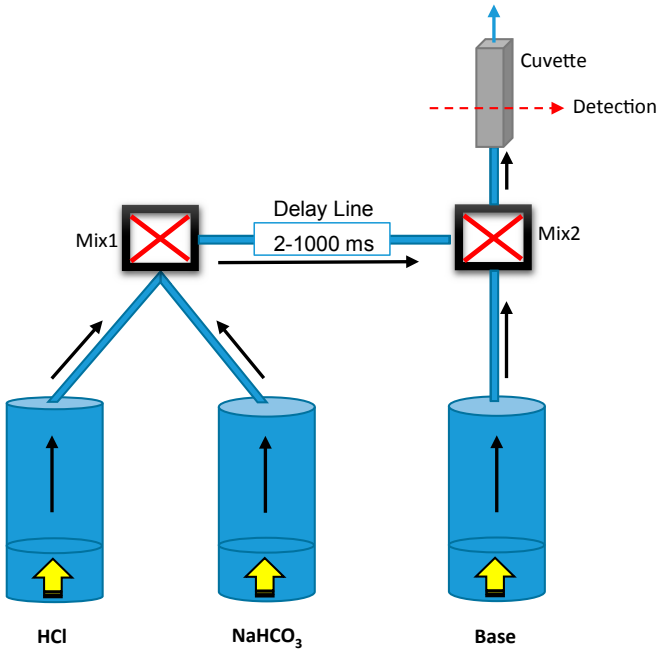

Fig. 5. The 2-stage stopped-flow setup used for the determination of CA's ability to protonate bases as shown in Fig. 2. In the first cell (*Top Left*), CA was generated by rapid acidification by HCl of bicarbonate anion HCO_3^-, resulting in a buffered solution with known pH. Following a variable incubation (delay) time during which there is a partial loss of CA due to spontaneous decomposition (Eq. **1**), the resulting CA solution was mixed in the second mixing cell (*Right*) with the base solution, allowing protonation of the base by CA. Temperature was controlled to within ± 0.1 °C by a variable-temperature water circulator. The concentration of the protonated base was measured by absorption spectroscopy.

readily available for these tasks with high kinetic efficiency. The nonvanishing presence of this small, mobile (neutral) carboxylic acid—which is strong enough to rapidly protonate practically all protonatable basic groups in human blood which then continue to react in their acid form—should not be ignored or marginalized.

Our findings also unveil the outstanding advantage of nature's choice of the CA buffer as its leading buffer: Dynamically, CA is a much stronger acid than all of the secondary buffers in the blood plasma. As such, CA acts as a fast-release proton storage with an overall bimolecular protonation rate of typical biological bases much larger than $(H^+)_{aq}$'s. CA has a further advantage: it would be able to directly protonate weak biological bases such as histidine [pK_a (H^+B) = 6.0] that are slow to protonate by secondary mobile buffers constructed with acids much weaker than CA; examples include $H_2PO_4^-$ (pK_a = 6.8), peptides, small proteins with pK_as in the 6 through 9-pK_a range, and carboxylate side groups with typical pK_a values of 4 to 6 such as in the important drug Ibuprofen. Such drug molecules may be transiently protonated by the stronger CA while diffusing in the blood plasma (60). Clearly, further investigations are needed to fully assess CA's physiological importance. It should be revealing to determine how CA reacts and protonates biorelevant bases in environments other than pure water. We expect that in such environments—especially in aprotic polar ones such as pure DMSO—CA will become much more stable, with its lifetime increasing from the millisecond to the second range. In such environments CA's direct protonation efficiency should remain high. Our preliminary experiments indicate the validity of these expectations.

Methods

Stopped-flow UV-visible experiments were performed using a BioLogic SFM-3000 stopped-flow spectrometer (Bio-Logic SA).

The stopped-flow, 2-stage rapid-mixing experimental investigation (Fig. 5) was carried out as follows. In the apparatus' first mixing cell, CA was transiently generated by mixing HCl with sodium bicarbonate $NaHCO_3$. The solution in the mixing cell where CA was prepared was incubated and allowed to fully equilibrate in the mixing cell (1-ms mixing time) for at least 2 ms and up to 1 s before the intact CA was mixed with, and protonated the base in, the base solution in the second mixing cell. Longer incubation times resulted in CA appreciably decomposing to CO_2 and H_2O prior to reacting with the base: The longer the incubation time, the more the CA's initial concentration was reduced by its decomposition in the first mixing stage.

For these 2-stage mixing experiments, the first mixing stage is described in *SI Appendix* for the conventional 1-step mixing experiments, while the second stage involved mixing of CA and 1 of the 2 representative bases, the HPTS or 1N4S basis. The base's UV-VIS absorption served as its concentration indicator. When mixed with the base in the second mixing chamber, the base protonation reaction was completed practically instantaneously on the 1-ms mixing timescale, and this protonation reaction is governed by the CA concentration at the time of mixing established by the incubation time in the first chamber where CA was generated.

ACKNOWLEDGMENTS. This work has been supported by NIH Grant PO 1000125420 (J.T.H. and E.P.).

1. C. L. Markert, F. Møller, Multiple forms of enzymes: Tissue, ontogenetic, and species specific patterns. *Proc. Natl. Acad. Sci. U.S.A.* **45**, 753–763 (1959).
2. A. Warshel, S. Russell, Theoretical correlation of structure and energetics in the catalytic reaction of trypsin. *J. Am. Chem. Soc.* **108**, 6569–6579 (1986).
3. H. J. Adrogué, N. E. Madias, Assessing acid-base status: Physiologic versus physicochemical approach. *Am. J. Kidney Dis.* **68**, 793–802 (2016).
4. M. Lee, C. Bai, M. Feliks, R. Alhadeff, A. Warshel, On the control of the proton current in the voltage-gated proton channel Hv1. *Proc. Natl. Acad. Sci. U.S.A.* **115**, 10321–10326 (2018).
5. W. Junge, S. McLaughlin, The role of fixed and mobile buffers in the kinetics of proton movement. *Biochim. Biophys. Acta* **890**, 1–5 (1987).
6. R. D. Vaughan-Jones, K. W. Spitzer, P. Swietach, Spatial aspects of intracellular pH regulation in heart muscle. *Prog. Biophys. Mol. Biol.* **90**, 207–224 (2006).
7. R. F. Schmidt, G. Thews, Eds., *Human Physiology* (Springer-Verlag, Berlin, 1980).
8. A. Waugh, A. Grant, *Anatomy and Physiology in Health and Illness* (Churchill Livingstone Elsevier, ed. 10, 2007), pp. 22.
9. C. Geers, G. Gros, Carbon dioxide transport and carbonic anhydrase in blood and muscle. *Physiol. Rev.* **80**, 681–715 (2000).
10. F. J. Millero, The marine inorganic carbon cycle. *Chem. Rev.* **107**, 308–341 (2007).
11. J. Fietzke *et al.*, Century-scale trends and seasonality in pH and temperature for shallow zones of the Bering Sea. *Proc. Natl. Acad. Sci. U.S.A.* **112**, 2960–2965 (2015).
12. K. Maher, C. P. Chamberlain, Hydrologic regulation of chemical weathering and the geologic carbon cycle. *Science* **343**, 1502–1504 (2014).
13. J. Hansen, M. Sato, Greenhouse gas growth rates. *Proc. Natl. Acad. Sci. U.S.A.* **101**, 16109–16114 (2004).
14. M. Tresguerres, T. J. Hamilton, Acid-base physiology, neurobiology and behaviour in relation to CO_2-induced ocean acidification. *J. Exp. Biol.* **220**, 2136–2148 (2017).
15. N. R. Mollica *et al.*, Ocean acidification affects coral growth by reducing skeletal density. *Proc. Natl. Acad. Sci. U.S.A.* **115**, 1754–1759 (2018).
16. V. C. Scanlon, T. Sanders, *Essentials of Anatomy and Physiology* (F.A. Davis Company, ed. 7, 2003).
17. G. A. Thibodeau, K. T. Patton, *Anatomy and Physiology* (Mosby, St. Louis, ed. 17, 2003).
18. D. N. Silverman, R. McKenna, Solvent-mediated proton transfer in catalysis by carbonic anhydrase. *Acc. Chem. Res.* **40**, 669–675 (2007).
19. C. T. Supuran, Structure and function of carbonic anhydrases. *Biochem. J.* **473**, 2023–2032 (2016).
20. R. K. Dash, J. B. Bassingthwaighte, Simultaneous blood-tissue exchange of oxygen, carbon dioxide, bicarbonate, and hydrogen ion. *Ann. Biomed. Eng.* **34**, 1129–1148 (2006).
21. N. M. Mangan, A. Flamholz, R. D. Hood, R. Milo, D. F. Savage, pH determines the energetic efficiency of the cyanobacterial CO_2 concentrating mechanism. *Proc. Natl. Acad. Sci. U.S.A.* **113**, E5354–E5362 (2016).
22. J. P. Wagner *et al.*, Tunnelling in carbonic acid. *Chem. Commun. (Camb.)* **52**, 7858–7861 (2016).
23. G. A. Mills, H. C. Urey, The kinetics of isotopic exchange between carbon dioxide, bicarbonate ion, carbonate ion and water1. *J. Am. Chem. Soc.* **62**, 1019–1026 (1940).
24. F. J. W. Roughton, The kinetics and rapid thermochemistry of carbonic acid. *J. Am. Chem. Soc.* **63**, 2930–2934 (1941).
25. C. Ho, J. M. Sturtevant, The kinetics of the hydration of carbon dioxide at 25 degrees. *J. Biol. Chem.* **238**, 3499–3501 (1963).
26. B. H. Gibbons, J. T. Edsall, Rate of hydration of carbon dioxide and dehydration of carbonic acid at 25 degrees. *J. Biol. Chem.* **238**, 3502–3507 (1963).
27. A. L. Soli, R. H. Byrne, CO_2 system hydration and dehydration kinetics and the equilibrium CO_2/H_2CO_3 ratio in aqueous NaCl solution. *Mar. Chem.* **78**, 65–73 (2002).
28. X. Wang, W. Conway, R. Burns, N. McCann, M. Maeder, Comprehensive study of the hydration and dehydration reactions of carbon dioxide in aqueous solution. *J. Phys. Chem. A* **114**, 1734–1740 (2010).
29. M. T. Nguyen, G. Raspoet, L. G. Vanquickenborne, P. T. Van Duijnen, How many water molecules are actively involved in the neutral hydration of carbon dioxide? *J. Phys. Chem. A* **101**, 7379–7388 (1997).
30. T. Loerting *et al.*, On the surprising kinetic stability of carbonic acid (H_2CO_3). *Angew. Chem. Int. Ed. Engl.* **39**, 891–894 (2000).
31. C. S. Tautermann *et al.*, Towards the experimental decomposition rate of carbonic acid (H_2CO_3) in aqueous solution. *Chemistry* **8**, 66–73 (2002).
32. M. Lewis, R. Glaser, Synergism of catalysis and reaction center rehybridization. A novel mode of catalysis in the hydrolysis of carbon dioxide. *J. Phys. Chem. A* **107**, 6814–6818 (2003).
33. P. P. Kumar, A. G. Kalinichev, R. J. Kirkpatrick, Dissociation of carbonic acid: Gas phase energetics and mechanism from ab initio metadynamics simulations. *J. Chem. Phys.* **126**, 204315 (2007).
34. M. T. Nguyen *et al.*, Mechanism of the hydration of carbon dioxide: Direct participation of H_2O versus microsolvation. *J. Phys. Chem. A* **112**, 10386–10398 (2008).
35. D. Marx, Proton transfer 200 years after von Grotthuss: Insights from ab initio simulations. *ChemPhysChem* **7**, 1848–1870 (2006).
36. A. Weller, Fast reactions of excited molecules. *Progr. React. Kinet.* **1**, 187–214 (1961).
37. M. Eigen, Proton transfer, acid-base catalysis, and enzymatic hydrolysis. Part I: Elementary processes. *Angew. Chem. Int. Ed. Engl.* **3**, 1–19 (1964).
38. M. Eigen, W. Kruse, G. Maass, L. DeMaeyer, Rate constants of protolytic reactions in aqueous solution. *Prog. React. Kinet.* **2**, 285–318 (1964).
39. M. Eigen, G. G. Hammes, "Elementary steps in enzyme reactions (as studied by relaxation spectrometry)" in *Advances in Enzymology and Related Areas of Molecular Biology*, F. F. Nord, Ed. (John Wiley & Sons, Inc., 1963), pp. 1–38.
40. J. N. Brønsted, Some observations about the concept of acids and bases. *Recl. Trav. Chim. Pays Bas* **42**, 718–728 (1923).
41. K. Adamczyk, M. Prémont-Schwarz, D. Pines, E. Pines, E. T. Nibbering, Real-time observation of carbonic acid formation in aqueous solution. *Science* **326**, 1690–1694 (2009).
42. D. Pines *et al.*, How acidic is carbonic acid? *J. Phys. Chem. B* **120**, 2440–2451 (2016).
43. P. Atkins, J. de Paula, *Physical Chemistry* (Oxford University, Oxford, ed. 9, 2010).
44. M. H. Kim, C. S. Kim, H. W. Lee, K. Kim, Temperature dependence of dissociation constants for formic acid and 2,6-dinitrophenol in aqueous solutions up to 175 °C. *J. Chem. Soc., Faraday Trans.* **92**, 4951–4956 (1996).
45. H. S. Harned, R. W. Ehlers, The dissociation constant of acetic acid from 0 to 60° centigrade. *J. Am. Chem. Soc.* **55**, 652–655 (1933).
46. H. S. Harned, N. D. Embree, The temperature variation of ionization constants in aqueous solutions. *J. Am. Chem. Soc.* **56**, 1050–1053 (1934).
47. H. S. Harned, B. B. Owen, *The Physical Chemistry of Electrolyte Solutions* (Reinhold, New York, ed. 3, 1958).

48. K. F. Wissbrun, D. M. French, A. Patterson, The true ionization constant of carbonic acid in aqueous solution from 5 to 45°. *J. Phys. Chem.* **58**, 693–695 (1954).
49. M. Tanaka, H. Nomura, F. Kawaizumi, A simple method for evaluation of enthalpy of proton dissociation in water. *Bull. Chem. Soc. Jpn.* **65**, 410–414 (1992).
50. E. Pines, B. Z. Magnes, M. J. Lang, G. R. Fleming, Direct measurement of intrinsic proton transfer rates in diffusion-controlled reactions. *Chem. Phys. Lett.* **281**, 413–420 (1997).
51. O. F. Mohammed, D. Pines, E. Pines, E. T. J. Nibbering, Aqueous bimolecular proton transfer in acid-base neutralization. *Chem. Phys.* **341**, 240–257 (2007).
52. P. M. Kiefer, J. T. Hynes, Nonlinear free energy relations for adiabatic proton transfer reactions in a polar environment. I. Fixed proton donor–acceptor separation. *J. Phys. Chem. A* **106**, 1834–1849 (2002).
53. P. M. Kiefer, J. T. Hynes, Nonlinear free energy relations for adiabatic proton transfer reactions in a polar environment. II. Inclusion of the hydrogen bond vibration. *J. Phys. Chem. A* **106**, 1850–1861 (2002).
54. E. Pines, "UV-visible spectra and photoacidity of phenols, naphthols and pyrenols" in *Chemistry of Phenols*, Z. Rappoport, Ed. (Wiley, New York, 2003), pp. 491–529.
55. M. Prémont-Schwarz, T. Barak, D. Pines, E. T. J. Nibbering, E. Pines, Ultrafast excited-state proton-transfer reaction of 1-naphthol-3,6-disulfonate and several 5-substituted 1-naphthol derivatives. *J. Phys. Chem. B* **117**, 4594–4603 (2013).
56. A. L. Lehninger, *Biochemistry* (Worth Publishers, New York, 1976).
57. S. Daschakraborty *et al*., Reaction mechanism for direct proton transfer from carbonic acid to a strong base in aqueous solution I: Acid and base coordinate and charge dynamics. *J. Phys. Chem. B* **120**, 2271–2280 (2016).
58. S. Daschakraborty *et al*., Direct proton transfer from carbonic acid to a strong base in aqueous solution II: Solvent role in reaction path. *J. Phys. Chem. B* **120**, 2281–2290 (2016).
59. S. Z. Fisher *et al*., Speeding up proton transfer in a fast enzyme: Kinetic and crystallographic studies on the effect of hydrophobic amino acid substitutions in the active site of human carbonic anhydrase II. *Biochemistry* **46**, 3803–3813 (2007).
60. C. D. Herzfeldt, R. Kümmel, Dissociation constants, solubilities and dissolution rates of some selected nonsteroidal antiinflammatories. *Drug Dev. Ind. Pharm.* **9**, 767–793 (1983).